

PERFORMANCE IMPROVEMENT OF SOLAR DRYER USING AN AUXILIARY HEAT SOURCE UNDER DIFFERENT VALUES OF AIRFLOW RATES

Alkahdery L.A.¹, Yurchenko A.V.², Mohammed J.A.-K.³, Mekhtiyev A.D.⁴, Neshina Y.G.^{5*}

¹ National Research Tomsk Polytechnic University, Tomsk, Russia

² National Research Tomsk State University, Tomsk, Russia

³ Electromechanical Engineering Dept., University of Technology, Baghdad, Iraq

⁴ S. Seifullin Kazakh Agrotechnical University, Astana, Kazakhstan

⁵ A. Saginov Karaganda Technical University, Karaganda, Kazakhstan, 1_neg@mail.ru

One of the most crucial methods for preserving agricultural produce is solar drying. The major focus of this paper is increasing solar drying systems' effectiveness. The development of new methods and variables that may have an impact on the functionality of solar dryers aids in enhancing their efficiency. An indirect-type solar dryer for drying agricultural products is proposed and developed in this study. A dryer consisting of a solar flat plate air collector, an insulated drying chamber, an auxiliary (electric) heat source, and an electric fan is constructed to improve the dryer's performance. The dryer's most typical function is to blow hot air at the product, forcing the water in it to evaporate. The effect of air temperature and velocity on evaporation rate has been studied experimentally. Tests with three different airflow rates—0.042, 0.0735, and 0.105 m³/s—are conducted. When there is little or no solar radiation, an auxiliary heater is used to provide sufficient heat. For varying airflow rates, solar mode and electrical mode were tested experimentally with only one energy source in each mode. The findings revealed that using a different heat source in addition to solar radiation will allow you to keep the air temperature in the drying chamber between 32 °C and 42°C. Also, it was found that for the whole drying process at high air velocities, the temperature had less influence on the dryer's performance.

Keywords: Solar dryer; auxiliary heat source; moisture content; solar air collector; airflow rate, PCB.

Introduction

The solar dryer enters many applications and the most important one is the food applications [1]. Drying is said to be the earliest method of preserving agricultural produce. The moisture content is lowered to its saturation level using this procedure. A heated air stream is blown across the product, either naturally or artificially, to create a moisture concentration gradient, causing moisture to move from the product's inside to its outside. Temperature variations that are above or below the allowed range induce physical and chemical changes, which eventually degrade the dried product's quality. Because most of the water content is dehydrated, providing air at a controlled temperature improves their storage life, decreases loss, and lowers costs of transportation [2–4].

The most crucial parameter that directly affects the drying rate is the temperature within the drying chamber. The major problem with a traditional solar dryer that doesn't have an auxiliary heat source is that solar energy is unpredictable. Nevertheless, the temperature threshold of drying air is greatly influenced by changing weather conditions and the intermittent nature of solar radiation. Hence, the quality of the dried product diminishes dramatically. As a result, without the presence of another energy source and complete control over all drying parameters, solar dryers are restricted and worthless.

Auxiliary heat of various forms can be used to augment solar energy and reduce drying time even further. During the various phases of the drying process, it is frequently beneficial to alter the rate of airflow passing through the drying system. There's also an auxiliary heating coil for use at night and on wet or cloudy days. Many different techniques of auxiliary heat have been used as complementary tools in the literature. Boughali et al. [5] developed a prototype of an energy-efficient indirect active hybrid solar-electric drier for agricultural goods. Song and Songlin [6] built a hybrid solar dryer that included a heat storage device and supplementary electricity heating. Mortezapour et al. created a hybrid photovoltaic-thermal solar dryer [7].

To ensure a continued drying process and the flexibility to operate the solar dryer under poor weather conditions, Zoukit et al. [8] employed a solar-gas collector in combination with an auxiliary heat system. By formatting the operation of a proportional valve, a control system is required to adjust the gas flow in the injector. Eltief et al. [9] employed a drying chamber, V-groove collectors, two variable-speed centrifugal fans, and an auxiliary electric heater as part of a solar-assisted drying system.

For rice drying, Zomorodian et al. [10] proposed a rig that included six standard solar air heaters, a drying chamber with an electrically rotational discharge valve, an auxiliary electric heating channel, and an air distribution system. During instances of low sunlight, Bennamoun and Belhamri [11] utilized a heater to dry onions. The most essential criteria that impact the dried product quality are the mass flow rate, temperature, and humidity of the air [12,13]. The performance of a solar-only dryer and another solar dryer with an auxiliary heater as a complement to the solar heat is investigated in an experimental study. Khalifa and Al-Dabagh [14] experimentally studied the effectiveness of a solar drying system that uses two flat plate collectors, a blower, and a drying chamber was experimentally tested with and without an auxiliary heater to augment the solar heat, and its performance was compared to that of natural drying. Four distinct airflow rates are used in the tests, namely 0.0383, 0.05104, 0.0638, and 0.07655 m³/s. The drying time was seen to have been cut from 56 hr for natural drying to 12–14 hr for sun drying and to 8–9 hr for combined (solar and auxiliary) drying. As compared to a system that uses only solar energy for drying, it was discovered that the combined system's efficiency increased by 25–40%. Krokida et al. [15] investigated how air drying of different plant materials (potato, carrot, pepper, garlic, mushroom, onion, leek, pea, maize, celery, pumpkin, and tomato) affected the drying kinetics and characteristic sample size. The equilibrium moisture content of dried goods within the range of 0.10–0.90 water activity at two temperatures (30 and 70 °C) was fitted to the GAB equation using a first-order reaction kinetics model. The drying sample size and air conditions were shown to have a significant impact on the model parameters under consideration. In instance, the temperature rise lowers the equilibrium moisture content of the dehydrated items and raises the drying constant.

During thin-layer drying of figs, Babalis and Belessiotis [16] investigated the effect of drying circumstances on the moisture diffusivity and drying constants and found that air velocities larger than 2 m/s had no considerable influence on the drying rate. The air temperature has the greatest impact on the drying kinetics, according to the findings. Purta and Abed [17] built and tested a solar dryer that consists of three main components: a drying sun collector, a solar dryer chamber, and a chimney. A fan was fitted at the chimney outlet to manually expel the hot air outside the solar dryer to boost drying efficiency.

In Basrah province, theoretical and practical research was undertaken by Al-Hilphy et al. [18] for the vacuum solar dryer, who was locally made to dry salted and unsalted carp fish, and it was compared to natural sun drying and vacuum electric dryer. It was found that the moisture content of dried fish dried using a vacuum solar dryer and a vacuum electric dryer were similar, although it was much better than sun-drying.

Ajiwiguna [19] experimented to find the impact of air temperature and velocity on evaporation rate. According to the findings, the impact of temperature is less important at high air speed. Suherman et al. [20] investigated the seaweed drying performance of a hybrid solar dryer combined with an auxiliary heater. Hybrid sun drying and conventional drying were both used to dry the samples. El Ferouali et al. [21] developed a new hybrid solar-electric dryer in which an electric auxiliary heater was put within the drying chamber to provide temperature control. Silva et al. [22] used the Photovoltaic PV system to power the blowers and the electric heater to provide a long-term drying solution. The maize grains were dried from 23 % moisture to 13 % moisture in 8.5 hours, with an average thermal and drying efficiency of 27 % and 6%, respectively.

Jadallah et al. [23] proposed a developed computational and experimental design of a hybrid PV Thermal double-pass counterflow system connected with a mixed-mode solar dryer system. The temperature of the solar cells was reduced by manually pumping air into the Photovoltaic thermal PVT system via a fan-created by the PV module, hence increasing the PV module's electrical efficiency. The air is passed from the fan to the PVT solar system, then into the drying chamber, using the forced convection mode.

The majority of previous studies have concentrated on the possibility of improving the solar dryer's efficiency by utilizing an extra heat source. A backup heater and variable airflow rates are employed to build an indirect solar dryer for large-scale agricultural drying, with solar mode (energy provided exclusively by solar energy) and electrical mode (energy provided solely by electrical power) dominated by a control system. When the temperature and relative humidity in the drying chamber change, the control system adjusts the amount of auxiliary heating and airflow as needed as a backup to solar energy.

In the present study, an indirect type solar dryer was proposed and developed to improve the drying process of agricultural products such as (banana). The dryer consists of a solar air collector, an isolated drying chamber, an auxiliary (electric) heat source, and an electric fan to drive the hot air according to the temperature and moisture in the dryer chamber. The most common function of the dryer is to blow hot air onto the product, forcing the water in it to evaporate. The effect of air temperature and velocity on the evaporation rate will be studied experimentally. The tests will be conducted at three different air flow rates. For variable air flow rates, the solar mode and the electric mode were experimentally tested with only one power supply in each mode.

1. Experimental system setup

The experimental setup includes a flat plate air solar collector and an indirect solar dryer with forced convection mode, as illustrated in Fig. 1, with external methods, such as a cross-flow cooling fan, for transporting solar energy in the form of hot air from the solar collector to the drying chamber. Between the absorber plate and the glass, heated air is transmitted. To optimize solar radiation exposure, the solar collector is affixed to a support structure that is inclined at a 30° angle to the horizon and faces south. Drying air enters the chamber directly after leaving the solar collector through a rectangular opening (Air Intake) with dimensions of $(0.7 \text{ m} \times 0.06 \text{ m})$. The underside of the constructed drying chamber is connected to an electrical heater ($220\text{V } 4\text{kW}$, accuracy $\pm 2\%$) acting as an auxiliary source.

The air passes through the trays from the bottom to the top. The drying chamber is made of galvanized iron plate measuring $(1.50 \text{ m} \times 0.87 \text{ m} \times 0.87 \text{ m})$ in dimension. The products are entered through an insulated door and mounted on the trays inside the drying cabinet. There are three trays, each with a dimension of $0.85 \text{ m} \times 0.65 \text{ m}$. The trays are made up of Plastic wire mesh having a thickness of 0.004 m and surrounded by a wooden frame. The sidewalls, bottom, and door of the drying chamber are made of two layers of steel (2 mm thick) separated by a polyurethane insulating foam layer (5 cm thick).

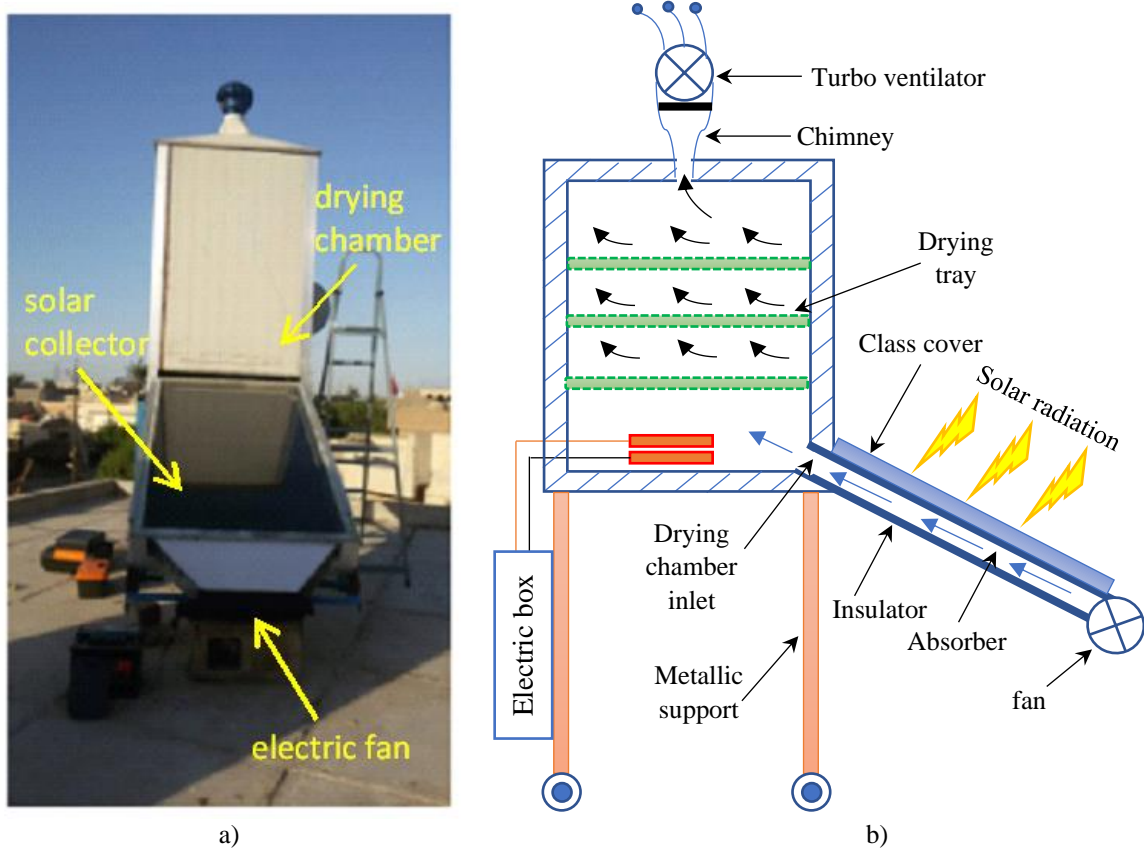


Fig. 1. Experimental set-up: a) photographic image and b) a schematic diagram of the solar dryer.

The distance between the lowest tray and the solar drying chamber's base is 0.40 m , with a gap of 0.15 m between each tray. When the sun goes down, an auxiliary backup heater is employed to assist this system

to replace solar energy. In both circumstances, the fan continues to function in line with the drying environment and uniform hot air circulation throughout the chamber. The flow of heated air within the drying chamber causes the drying process to take place.

2. System implementation procedure

Experiments on drying were carried out in October 2020 from 7:00 a.m. to 5:00 p.m., with solar radiation as the heat source. The next day, from 5:00 p.m. until 7:00 a.m., a new source was added to the drying system. The tests were implemented in Baghdad, Iraq (latitude 33.333 and longitude 44.433) on days with a clear sky on the 21, 22, and 23 October, respectively. For both heating modes, several experiments were implemented on the systems utilizing varying airflow rates of 0.042, 0.0735, and 0.105 m³/s. In the drying experiments, fresh banana slices were used. Banana slices, with a thickness of 4–5 mm, were chosen for optimal drying.

The reduction in moisture content was calculated by weighing the product sample every hour. The system must first be brought to steady-state conditions before the tests can begin. As a result, each test run must be preceded by an operating period of at least 1 hour. The (SM206-SOLAR) solar meter was employed to measure the global components of solar radiation in real-time. Also, the temperature of the collector inlet and outlet, the temperature of the absorber plate, the temperature of the exterior glass cover, the temperature of the drying chamber inlet and outlet, and the temperature of the product were all measured using a Lutron (TM – 903 A) four-channel temperature data logger.

A TES-1341 hot-wire anemometer relative humidity was used to measure the relative humidity of the ambient air and the entrance of the drying chamber. The air speed was measured by using wind speed (UNI-T UT362 anemometer with USB). To acquire the average value of air speed, the air exit speed was measured at three positions in the exit air throat of the aperture area at the top of the drying chamber. The average speed could be used in determining the air density and cross-section area of the aperture area and the air mass flow rate. All specifications of the measuring devices are listed in Table 1.

Table 1. The specifications of measuring instruments

Instrument	Accuracy	Range	Resolution
SM206-SOLAR Solar irradiation meter	±5% of reading	1-3999 w/m ² (btu)	0.1 W/m ²
Lutron (TM – 903 A), 4 channels temperature data logger	± (0.5 % + 1 °C)	- 100 °C to 1300 °C	0.1 ° C.
Lutron HT-3007SD Humidity/Temperature Meter	3% reading + 1% RH., 0 to 50°C	5 % to 95 % R.H., ± 0.8°C	0.1 % R.H., 0.1 degree
TES-1341 HOT-WIRE ANEMOMETER relative humidity	±3% RH	10% to 95%	±3%RH
UNI-T UT362 anemometer with USB	(± 3%+5)	2~10 m/s	-----

3. Analysis of dryer performance

The moisture content is computed using the equation below:

$$M = \frac{W_o - W_d}{W_o} \times 100, \quad (1)$$

where M is the moisture content (g water/g dry solid), W_o is the initial weight of undried product (g), W_d is the weight of dry matter in produce (g).

Many factors impact the effectiveness of a flat plate collector, including the collector's size, geographic location, velocity, humidity, and ambient air temperature, among others. The solar collector's thermal efficiency is calculated as follows:

$$\eta_c = \frac{m_a C_{pa} (T_{oc} - T_{ic})}{A_c I}. \quad (2)$$

Here η_C is the efficiency of solar collector, m_a is the air mass flow rate (kg/s), C_{pa} is the air specific heat (kJ/kgK), T_{oc} is the Exit air temperature of collector (°C), T_{ic} is the input air temperature of collector (°C), A_c is the area of collector (m^2), and I is the global solar radiation (W/m^2).

The solar collector's thermal efficiency was determined to be 28% for average solar radiation of 600 W/m^2 and average input and exit air temperatures of 31°C and 45°C, respectively. The thermal efficiency of the solar dryer system can be calculated as follows [24].

$$\eta_d = \frac{m_w h_l}{A_c I t}, \quad (3)$$

The efficiency of the heater is determined as:

$$\eta_h = \frac{m_a C_{pa} (T_{oc} - T_{ic})}{I_e V}, \quad (4)$$

where η_d is the efficiency of the solar dryer (%), η_h is the efficiency of the heater (%), M_w is the mass of evaporated water (kg), h_l is the latent heat of vaporization (kJ/kg), t is the Solar drying time (hour), I_e is the electric current (A), and V is the voltage (V).

Understanding the performance parameters of solar dryers requires analyzing them. Depending on the current circumstances, which are dictated by the partial pressure vapors in the air and as well as the gradient of the vapor pressure of water contained in the product, a wet product exposed to the air stream may lose or acquire moisture. Assume that the vapor partial pressure in the air in a sample remains constant, we will arrive at a situation known as equilibrium moisture content after passing a stream of air through it for a long enough time (EMC). The EMC is affected by temperature, relative humidity, and the product's nature. These equilibrium moisture relationships are normally expressed mathematically. The equilibrium moisture content can be calculated as follows [25]:

$$\%RH = 1 - \exp(-K_t (EMC)^N), \quad (5)$$

where %HR is the equilibrium moisture content, K_t and N are constant, and EMC is the equilibrium moisture content.

3.1 Activity of water

The more water in a product, the better it is for microbial development, which affects shelf stability and safety. A banana's water activity is estimated to be (0.987–0.964) [26]. The following equation [27] can be used to calculate the water activity.

$$a_w = \frac{EMC}{100}, \quad (6)$$

where a_w is the Equation of water activity.

The difference in moisture content between the materials to be dried and the equilibrium moisture content is usually related to the drying rate. The drying rate is proportional to the change in moisture content between the items to be dried and the content of equilibrium moisture, according to the following equation [28]:

$$A_{dr} = \frac{m_o}{t_d}, \quad (7)$$

where A_{dr} is the Average drying rate (kg/hr), m_o is the Moisture mass removed by solar heat (g), and t_d is the Overall drying time (hour). The following equation [29] can be used to calculate the quantity of moisture to be extracted from the product, m_w :

$$m_w = m_i \left(\frac{M_i - M_f}{1 - M_f} \right), \quad (8)$$

where m_i is the initial mass of product to be dried (g), M_i is the Initial moisture content on a % wet basis, M_f is the final moisture content % wet basis.

4. Results and discussion

Throughout October 2020, several continuing experimental testing on the improved dryer were conducted. Figures 2 and 3 show the time variation of solar intensity (I), ambient temperature (T_a), inlet temperature (T_i), and outlet temperature (T_o) of air from the drying chamber, for three consecutive days on October 21, 22, and 23, 2020, with three different airflow rates of 0.042, 0.0735, and 0.105 m³/s, respectively. It is clear that all figures are a natural phenomenon and a clear fact based on the weather data at that location and these days of the year. Temperature changes are exactly related to intensity changes, as seen in the figures. In addition, there is a large difference in hot air and ambient temperature due to the collector's capacity to heat the surrounding air.

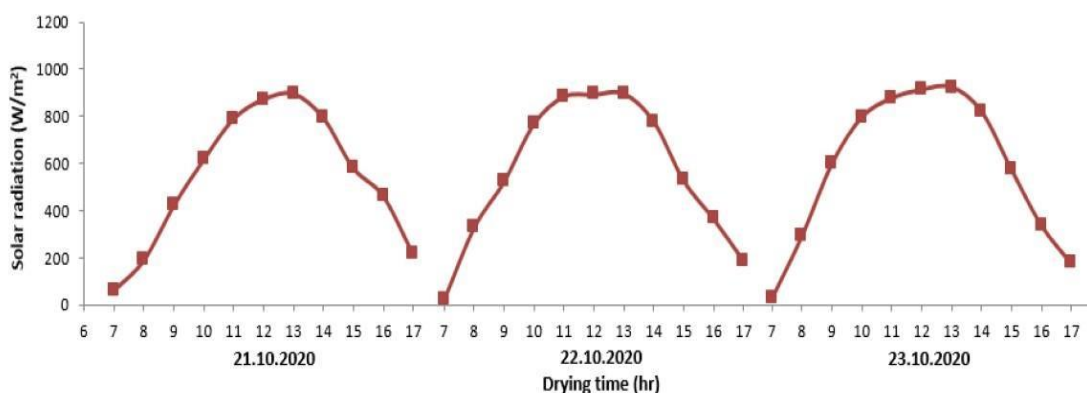


Fig. 2. Variation of the intensity of solar radiation (I) versus drying time

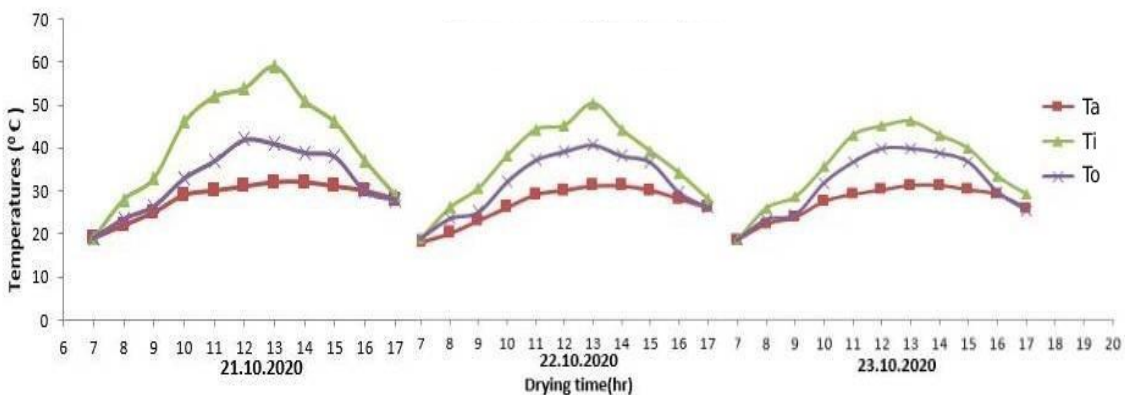


Fig. 3. Ambient temperature (T_a), drying chamber inlet air temperature (T_i), drying chamber outlet air temperature (T_o) versus drying time.

Fig. 4 demonstrates the variation of relative humidity with solar drying time for various airflows. It can be observed that relative humidity decreases as drying time rises, peaking at 13:00, before rising again at 17:00 for all airflows at the end of the sunny hours. It can be seen that the relative humidity is the lowest in the chamber dryer at airflow of 0.105 m³/s compared to the lowest values for airflows.

The speed of the air may not be sufficient to carry away the moisture from the material surface to the outside of the drying chamber, so the relative humidity of the air increases at low flow rates. Also, with a higher airflow of 0.105m³/s, relative humidity is very low in the drier, which is helpful for a faster drying rate since low humid air has a greater potential to absorb moisture. The most significant criteria for successful drying are a greater temperature and lower relative humidity.

Fig. 5 depicts the chamber temperature (T_r) as a function of overall drying time (t_d) under varied airflow rates. When applying an additional source (backup heater) to the dryer from 1 a.m. to sunrise at 5:23 a.m., the drying chamber temperature dropped slightly as drying time increased due to the low temperature of the ambient air.

The heater continues to heat the air until 7:30 a.m., after which the heater is shut off and only solar radiation is used to heat the air flowing over the solar collector's absorber surface. The radiation is low at the start of the day, gradually increasing until it peaks at midday, and then gradually decreasing until it reaches its lowest point at sunset. Throughout the day, the temperature rise is determined by the radiation levels. Due to the absence of solar radiation energy at sunset and the decreased ambient air temperature, a backup heater is employed once again. The temperature of the chamber decreases as the airflow rates increase in all three scenarios.

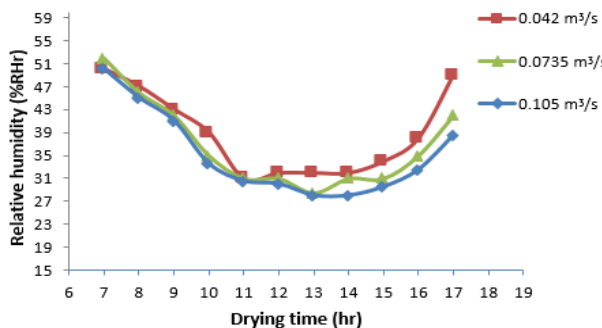


Fig. 4. The drying chamber humidity ratio vs. solar drying time under variable airflow rates

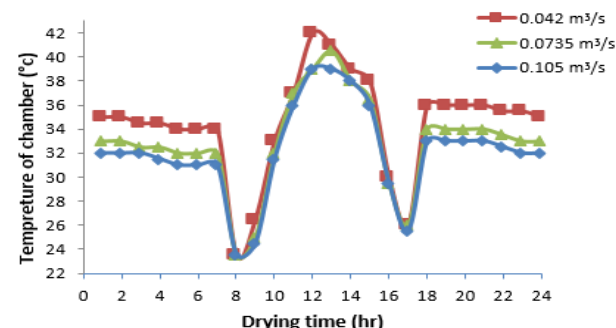


Fig. 5. Drying chamber temp. of (T_r) with auxiliary heat source vs. overall drying time (t_d) under variable airflow rates

Fig. 6 shows how larger airflows improve drying system efficiency because more air passes over the product perimeter, forcing water vapor to evaporate and therefore improving the drying rate. The drying system's efficiency improves as the airflow velocity rises. Fig. 7 depicts the relationship between moisture content and overall drying time for various airflow speeds. At the beginning of the drying curve, there is a constant drying rate, followed by a falling rate drying period. It's worth noting that the drying rate remains constant at the start of the drying curve before rapidly decreasing.

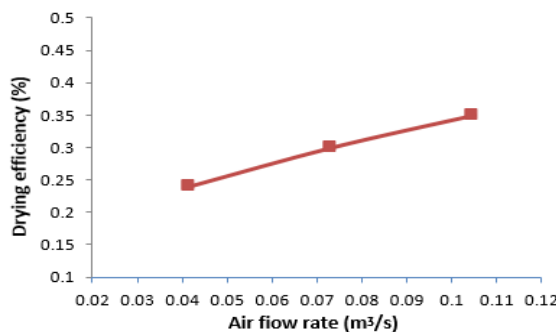


Fig. 6. Drying system efficiency vs. air flow rate

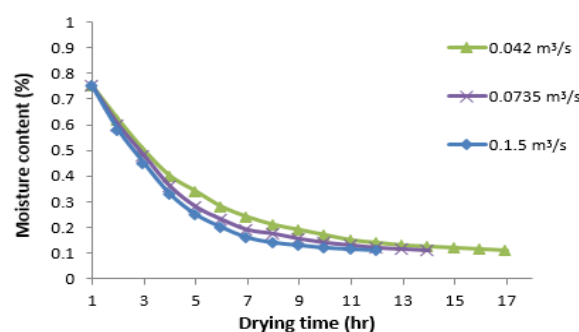


Fig. 7. Moisture content vs. overall drying time under variable airflow rates

Moisture will be removed by evaporation as air passes over the surface of banana slices, and moisture will be continuously transported from the inner portion of the slice to the surface in an attempt to maintain that moisture pool. Nevertheless, the surface moisture pool will eventually disappear. At this point, the dryer will start a decreasing rate drying period, in which moisture must diffuse from the material's core to the surface. The amount of water that evaporates steadily reduces over time in the lowest airflow used during measurements, even though the banana receives considerable heat. The impact of controlling air flow rate on sun drying time depends on the strength of solar radiation. In light of this, monitoring the dryer's functioning is made easier by the temperature and humidity measurements.

Conclusions

The performance of the solar dryer including an auxiliary heat source was evaluated in an experimental investigation with varying airflow speeds. From the results, some conclusions can be drawn as follows:

1. The air temperature in the range of 32–42 °C within the drying chamber may be maintained throughout the duration of the product drying by using an additional heat source in addition to sun radiation.
2. It's a good idea to use an electric fan and backup heater to improve the dryer's thermal performance. As a result, the proposed dryer is more effective and practical than the conventional solar dryer in drying and heating applications.
3. The proposed dryer speeds up the drying process (decrease in drying time) and thus minimizes humidity and spoilage risk, and increases product quality. This will significantly reflect on the performance efficiency.
4. Higher air temperatures have a considerable influence on the drying rate in the early stages of drying, but this effect decreases after around 10–15 hours.
5. Because it inhibits the creation of the stagnant boundary layer air, air velocity has a significant impact in the early stages of drying. This means that the air around the product will not be saturated, preventing steam from leaking into the surrounding air.
6. The maximum average drying efficiency was determined to be 35 % at a flow rate of 0.105 m³/sec, with average solar radiation of 600 W/m² and an average ambient temperature of 27.5°C, with a relative humidity of 35.136 % in the drying chamber.
7. The drying time at varied flow rates of 0.042, 0.0735, 0.105 m³/sec with a moisture content of 0.11 was 17, 14, 11.5 hours during daylight hours, respectively.

Funding (or Acknowledgments)

The study was supported by a grant from the Russian Science Foundation No. 22-19-00389,
<https://rscf.ru/project/22-19-00389/>.

REFERENCES

- 1 Mohana Y., Mohanapriya R., Anukiruthika T., Yoha K.S., Moses J.A., Anandharamakrishnan C. Solar dryers for food applications: Concepts, designs, and recent advances. *Solar Energy*. 2020, Vol. 208, pp. 321 – 344. doi:10.1016/j.solener.2020.07.098
- 2 Fudholi A., Sopian K., Ruslan, M.H., Sulaiman, M.Y. Review of solar dryers for agricultural and marine products. *Renew. Sustain. Energy Rev.* 2010, Vol.14, pp. 1–30. doi:10.1016/j.rser.2009.07.032
- 3 Afriyie J.K., Nazha M.A.A., Rajakaruna H., Forson F.K. Experimental investigations of a chimney-dependent solar crop dryer. *Renew. Energy*. 2009, Vol.34, pp. 217 – 222. doi:10.1016/j.renene.2008.04.010
- 4 Kumar R., Chauhan R., Sethi M., Sharma A., Kumar A. Experimental investigation of effect of flow attack angle and thermohydraulic performance of air flow in a rectangular channel with discrete V-pattern baffle on the heated plate. *Adv. Mech. Eng.* 2016, Vol.8, pp. 1–12. doi:10.1177/1687814016641056
- 5 Boughali S., Benmoussa H., Bouchekima B., Mennouche D., Bouguettaia H., Bechki D. Crop drying by indirect active hybrid solar-Electrical dryer in the eastern Algerian Septentrional Sahara, *Solar Energy*. 2009, Vol.81, No.12, pp. 2223–2232. doi:10.1016/j.solener.2009.09.006
- 6 Song M., Songlin Y., Biguang Z., Dong Z. Experimental Research of Grape Drying Using Solar Dryer with Latent Heat Storage System. *Int. Conf. on Computer Distributed Control and Intelligent Environmental Monitoring*. 2011, pp. 740 – 742. doi: 10.1109/CDCEIM.2011.33
- 7 Mortezapour H., Ghobadian B., Minaei S., Khoshtaghaza M.H., Mortezapour H., M.S. Saffron. Drying with a Heat Pump – Assisted Hybrid Photovoltaic – Thermal Solar Dryer, *Drying Technology*. 2012, Vol.30, No.6, pp. 37–41. doi:10.1080/07373937.2011.645261
- 8 Zoukit A., El Ferouali H., Salhi I., Doubabi S., Abdenouri N., El Kilali T. Control of a solar dryer using a hybrid solar gas collector. 2016 *Inter. Conf. on Elect. Sci. and Tech. in Mag. (CISTEM)*. doi:10.1109/CISTEM.2016.8066825
- 9 Eltief S.A., Ruslan M.H., Yatim B. Drying chamber performance of V-groove forced convective solar dryer. *Desalination*, 2007, Vol.209, No.1, pp. 151–155. doi:10.1016/j.desal.2007.04.024
- 10 Zomorodian A., Zare D., Ghasemkhani H. Optimization and evaluation of a semi-continuous solar dryer for cereals (Rice, etc). *Desalination*, 2007, Vol.209, No.1, pp. 129–135. doi:10.1016/j.desal.2007.04.021
- 11 Bennamoun, L. and Belhamri, A. Design and simulation of a solar dryer for agriculture products, *Journal of Food Engineering*. 2003, Vol.59, pp. 259–266. doi:10.1016/S0260-8774(02)00466-1

- 12 Chanakarn C. Drying by Producer Gas from an Up-Flow Gasifier. *Department of energy technology king Mongkut's University of Technology Thonburi*, 1991. <https://www.researchgate.net/publication/237134220>
- 13 Elston A.J. Rates of Water Vapour Adsorption from Air by Silica Gel. *Industrial and Engineering Chemistry*. 1939, Vol.31, No.8, pp. 988–992. doi:10.1021/ie50356a014
- 14 Khalifa A.N., Al-Dabagh A. An Experimental Study of Vegetable Solar Drying Systems with and without Auxiliary Heat. *ISRN Renewable Energy*, 2012, Vol.2012, pp. 1-8. doi:10.5402/2012/789324
- 15 Krokida M.K., Karathanos V.T., Maroulis Z.B., Marinos-Kouris D. Drying kinetics of some vegetable. *Journal of Food Engineering*, 2003, Vol.59, No.4, pp. 391-403. doi:10.1016/S0260-8774(02)00498-3
- 16 Babalis S.J., Belessiotis V.G. Influence of the drying conditions on the drying constants and moisture diffusivity during the thin-layer drying of figs. *J. of Food Eng.*, 2004, Vol.65, No.3, pp. 449-458. doi:10.1016/j.jfoodeng.2004.02.005
- 17 Abed E.M. Design and Testing Solar Dryer Performance. *Eng. and Tech. J.* 2013, Vol.31, No.12, pp. 169-184. doi:10.30684/etj.31.12A.14
- 18 Al-Hilphy A.R.S., Al-Shatty S.M.H., Gahffr A.A. A Practical and Theoretical Study of the Locally Manufactured Vacuum Solar Dryer for Fish Drying. *Eng. and Tech. J.* 2016, Vol.34, No.3, pp. 76-91. doi:10.30684/etj.34.3B.17
- 19 Purta R.N., Ajiwiguna T.A. Influence of Air Temperature and Velocity for Drying Process. *Procedia Engineering*. 2017, Vol.170, pp. 516 – 519. doi:10.1016/j.proeng.2017.03.082
- 20 Suherman S., Rizki H., Rauf N., Susanto E.E. Performance study of hybrid solar dryer with auxiliary heater for seaweed drying. *Journal of Physics: Conf. Series*. 2019, Vol.1295, No.012002. doi:10.1088/1742-6596/1295/1/012002
- 21 El Ferouali H., Zoukit A., Salhi I., El Kilali T., Doubabi S., Abdenouri N. Optimization study and design of a hybrid solar-electric dryer suitable to the developing countries context. *Solar for Africa and Renewable Energies Journal (SARE)*, V1-FEB19. 2019, pp. 35-39. <https://www.researchgate.net/publication/337496021>
- 22 Silva G.M., Ferreira A.G., Coutinho R.M., Maia C.B. Experimental Analysis of Corn Drying in A Sustainable Solar Dryer. *Journal of Advanced Research in Fluid Mechanics and Thermal Sciences*. 2020, Vol.67, No.2, pp. 1-12. <https://www.akademiabaru.com/submit/index.php/arfmts/article/view/3569>
- 23 Jadallah A.A., Alsaadi M.K., Hussien S.A. The Hybrid (PVT) Double-Pass System with a Mixed-Mode Solar Dryer for Drying Banana, *Eng. and Tech. J.* 2020, Vol.38, No.8, pp. 1214-1225. doi:10.30684/etj.v38i8A.535
- 24 Midilli A. Determination of pistachio drying behavior and conditions in a solar drying system, *International Journal of Drying Res.* 2001, Vol.25, No.8, pp. 715-725. doi:10.1002/er.715
- 25 Iglesias and Chirife, 1982; ASAE, 2000.
- 26 Chirife J., Fontan C.F. Water activity of fresh foods. *Journal of Food Science*. 1982, Vol.47, pp. 661-663. doi:10.1111/j.1365-2621.1982.tb10145.x
- 27 Barbosa-Cánovas G.V., Fontana A.J., Schmidt S.J., Labuza T.P. Water Activity in Foods: Fundamentals and Applications. *John Wiley & Sons*, 2020, Inc. ISBN:978-1-118-76831-0
- 28 Adelaja A.O., Babatope B.I. Analysis and Testing of a Natural Convection Solar Dryer for the Tropics. *Journal of Energy*. 2013, Vol.4, pp. 1-8. doi:10.1155/2013/479894
- 29 Moisture P.Y. Water Activity. *Handbook of Processed Meats and Poultry Analysis*. 2008, pp. 35-67. doi:10.1201/9781420045338.ch3.